EMBO Molecular Medicine

Apoptosis inhibitors and mini-agrin have additive benefits in congenital muscular dystrophy mice

*Sarina Meinen[1], Shuo Lin[1], Raphael Thurnherr[2], Michael Erb[3], Thomas Meier[3], Markus A. Rüegg[1]**

Keywords: cell death; extracellular matrix; laminin-211; merosin; muscle regeneration

DOI 10.1002/emmm.201100151

Received December 23, 2010
Revised April 29, 2011
Accepted May 17, 2011

Mutations in *LAMA2* cause a severe form of congenital muscular dystrophy, called MDC1A. Studies in mouse models have shown that transgenic expression of a designed, miniaturized form of the extracellular matrix molecule agrin ('mini-agrin') or apoptosis inhibition by either overexpression of Bcl2 or application of the pharmacological substance omigapil can ameliorate the disease. Here, we tested whether mini-agrin and anti-apoptotic agents act on different pathways and thus exert additive benefits in MDC1A mouse models. By combining mini-agrin with either transgenic Bcl2 expression or oral omigapil application, we show that the ameliorating effect of mini-agrin, which acts by restoring the mechanical stability of muscle fibres and, thereby, reduces muscle fibre breakdown and concomitant fibrosis, is complemented by apoptosis inhibitors, which prevent the loss of muscle fibres. Treatment of mice with both agents results in improved muscle regeneration and increased force. Our results show that the combination of mini-agrin and anti-apoptosis treatment has beneficial effects that are significantly bigger than the individual treatments and suggest that such a strategy might also be applicable to MDC1A patients.

INTRODUCTION

Laminin-α2-deficient congenital muscular dystrophy (MDC1A) is the most prevalent form of congenital muscular dystrophies. Patients suffer from severe muscle degeneration often leading to death in early childhood. Moreover, the disease is accompanied by a rather mild neuropathy that is based on the demyelination of the peripheral nerve (Miyagoe-Suzuki et al, 2000; Tome & Fardeau, 1998). On the cellular level, muscles of MDC1A patients are characterized by marked variation in muscle fibre size, extensive fibrosis and proliferation of adipose tissue. MDC1A is caused by mutations in *LAMA2*, the gene that encodes the laminin-α2 chain, which is an important component of the extracellular matrix of skeletal and heart muscle as well as peripheral nerve. In muscle, the most prevalent form of laminin that contains laminin-α2 is laminin-211 (LM-211), a heterotrimer consisting of the α2, the β1 and the γ1 chain. LM-211 is tightly attached to the basement membrane and interacts with α-dystroglycan and α7β1 integrin expressed on the muscle fibre surface (Colognato & Yurchenco, 2000). Laminin-α2 deficiency, therefore, disrupts the mechanical linkage between the basement membrane and the muscle fibre. In addition, there is evidence that the lack of LM-211 prevents activation of several signalling cascades (Langenbach & Rando, 2002; Laprise et al, 2003). Although skeletal muscle fibres of MDC1A patients and mouse models thereof show increased levels of LM-411, the α4 chain seems not to be sufficient to fully compensate for the loss of LM-211. The reason for this lack of compensation might be the failure of LM-411 to induce laminin self-polymerization and to bind to α-dystroglycan (Colognato & Yurchenco, 1999).

Despite the knowledge of molecular events underlying the disease, there are no treatments available to date (Collins & Bonnemann, 2010). Because the formation of basal lamina and receptor-mediated signalling are important in the maintenance of muscle, impairment of those functions probably determines

(1) Biozentrum, University of Basel, Basel, Switzerland
(2) Departments of Anaesthesia and Research, University of Basel Kantonsspital, Basel, Switzerland
(3) Santhera Pharmaceuticals, Liestal, Switzerland
***Corresponding author:** Tel: +41 61 267 2223, Fax: +41 61 267 2208; E-mail: markus-a.ruegg@unibas.ch

the severity of MDC1A. Consequently, several mechanisms contribute to the pronounced muscle wasting observed in MDC1A. First, the lack of extracellular matrix–cytoskeletal linkage and/or intracellular signalling results in the inability of muscle fibres to withstand the mechanical forces imposed on them during contraction and leads to their degeneration. Secondly, regeneration of skeletal muscle after injury has been shown to be abortive in mouse models for MDC1A (Bentzinger et al, 2005; Kuang et al, 1999; Meinen et al, 2007). Thirdly, apoptosis of myofibres was shown to contribute to the dystrophic phenotype of MDC1A mouse models (Bentzinger et al, 2005; Kuang et al, 1999; Miyagoe et al, 1997).

Agrin is an extracellular matrix molecule that is well known for its function to induce postsynaptic specializations at the neuromuscular junction (Bezakova & Ruegg, 2003). Alternatively spliced forms of agrin that are expressed in non-neuronal tissue, including muscle, lack this postsynapse-inducing activity but bind with very high affinity to laminins via their N-terminal end (Denzer et al, 1997) and to α-dystroglycan via their C-terminal part (Gesemann et al, 1998). These binding data indicate that agrin could potentially link LM-411 to α-dystroglycan and thus reverse the structural deficit of MDC1A muscle. Indeed, preclinical proof-of-concept studies in dy^W/dy^W mice, a well-characterized mouse model for MDC1A (Kuang et al, 1998b), have shown that overexpression of a miniaturized form of agrin (called mini-agrin) in skeletal muscle increased the tolerance of muscle to mechanical load and improved regeneration of muscle (Bentzinger et al, 2005; Moll et al, 2001) at any stage of the disease (Meinen et al, 2007). Mini-agrin was also successfully delivered to skeletal muscles by systemic application of adeno-associated viral vectors (Qiao et al, 2005).

Despite strong improvement, transgenic expression of mini-agrin did not remove all of the disease symptoms. The main reason for this is probably the lack of expression of mini-agrin in peripheral nerve and in the central nervous system, but only partial restoration of muscle function may also contribute. For example, mini-agrin is not known to bind to integrins and thus, any function mediated by the binding of LM-211 to integrins cannot be compensated for. Indeed, laminin interactions with integrins were shown to activate several pathways that prevent apoptosis (Burkin & Kaufman, 1999; Kuang et al, 1998a, 1998b; Laprise et al, 2002; Vachon et al, 1996, 1997). Interestingly, muscle-specific overexpression of the apoptosis inhibitor Bcl2 (Dominov et al, 2005) or deletion of the pro-apoptotic factor Bax (Girgenrath et al, 2004) significantly improved the dystrophic phenotype and muscle function, and prolonged lifespan in MDC1A mice. Moreover, the apoptosis inhibitors doxycycline and omigapil have been shown to affect disease course in dy^W/dy^W mice (Erb et al, 2009; Girgenrath et al, 2009). Because mutations in *LAMA2* cause a multitude of phenotypes that are based on LM-211 affecting multiple pathways, we now examined whether a combined treatment exerts additional benefits and could increase treatment efficacy.

In a first 'proof-of-concept' study, we generated dy^W/dy^W mice that overexpressed both mini-agrin and the apoptosis inhibitor protein Bcl2 in skeletal muscle. In a step towards application of a combined treatment, we also tested whether the orally bioavailable apoptosis inhibitor omigapil (*N*(dibenz(b,f)-oxepin-10-ylmethyl)-*N*-methyl-*N*-prop-2-ynylamine maleate), when combined with mini-agrin, would add further benefit. We report here that the combined treatment with mini-agrin and apoptosis inhibitors indeed provides additive benefit to single treatment on the disease progression in dy^W/dy^W mice. In particular, we show that mini-agrin prevents muscle degeneration due to mechanical load and thus reduces the replacement of muscle with fibrotic tissue, whereas, inhibition of apoptosis allows the muscle to maintain a near-normal number of fibres. Together, apoptosis inhibitors and mini-agrin potentiate the regeneration capacity and allow diseased muscle fibres to increase in diameter. Most importantly, the dual treatment resulted in a marked increase in muscle force.

RESULTS

Bcl2 and mini-agrin affect different parameters in muscle of dy^W/dy^W mice

To see whether inhibition of apoptosis and stabilization of the connection between basement membrane and muscle sarcolemma would have an additive benefit for the muscle disease, we mated heterozygous dy^W/wt mice with mice transgenic for Bcl2 (Dominov et al, 2005; Girgenrath et al, 2004) or mini-agrin (Moll et al, 2001). The resulting offsprings with the correct genotype were then further mated to eventually obtain mice that were deficient for laminin-α2 and transgenic for Bcl2 (called dy^W/Bcl), mini-agrin (dy^W/mag) or both transgenes (dy^W/Bcl/mag). To assure that expression of all transgenes was not altered by the genotype, protein levels were determined in the *triceps* muscle from mice with the different genotypes. Indeed, Bcl2 and mini-agrin were expressed at high levels in the transgenic mice as determined by Western blot analysis (Fig S1A of Supporting information).

To determine the effect of the transgenes on the muscle pathology, we analysed the fast-twitch foreleg muscle *triceps brachii* (Fig 1) and the slow-twitch hindleg muscle *soleus* (Fig 2). The latter becomes progressively paralysed in dy^W/dy^W mice as a consequence of peripheral nerve demyelination (Kuang et al, 1998b). Haematoxylin & Eosin (H & E; Merck) and Masson's trichrome stainings of *triceps* muscle of 12- (Fig 1A) and 16-week-old animals (Fig 1B) are shown. They revealed extensive fibrosis and a high proportion of small, rounded fibres in dy^W/dy^W mice (Fig 1A). Expression of mini-agrin (dy^W/mag) largely impeded the replacement of muscle with fibrotic tissue while Bcl2 expression (dy^W/Bcl) seemed to increase fibrosis in dy^W/dy^W muscle (Fig 1A), a finding that was confirmed by quantification of the relative fibrotic area (Fig 1C) and by determining the amount of the collagen-specific amino acid hydroxyproline, which is a measure of fibrosis (Fig S2A of Supporting information). However, co-expression of mini-agrin (dy^W/Bcl/mag) eliminated the fibrotic impact of Bcl2 (Fig 1A and C and Fig S2A of Supporting information). The high degree of fibrosis in Bcl2 transgenic dy^W/dy^W mice coincided with a strong increase in the number of macrophages in *triceps* of dy^W/Bcl mice (Fig S2C and D of Supporting information). Like

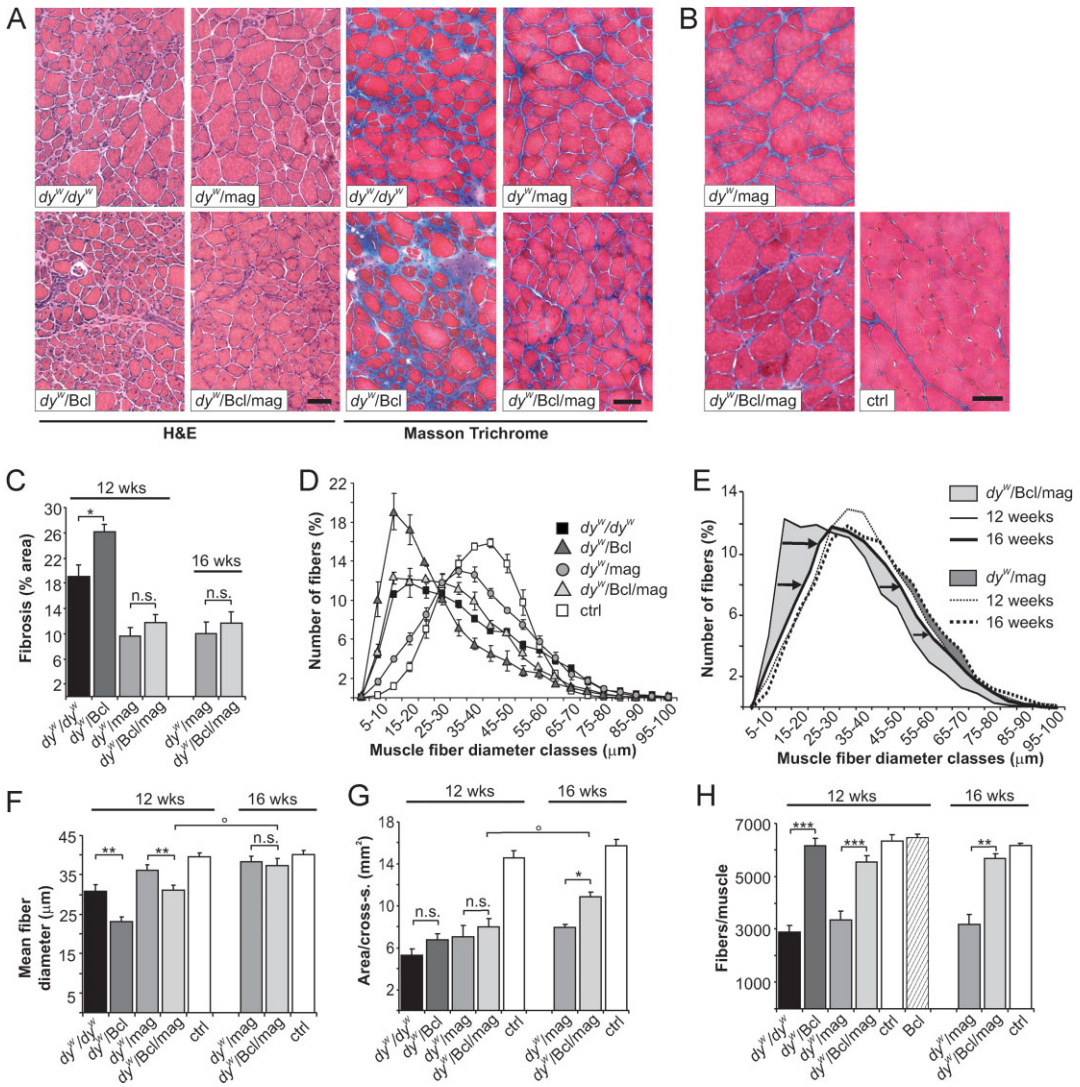

Figure 1. Histological analysis of *triceps brachii* muscle from 12- to 16-week-old mice.

A. H & E and Masson's trichrome staining of cross-sections from 12-week old mice.

B. Masson's trichrome staining from 16-week-old mice. Pathological changes observed in dy^W/dy^W mice, such as fibrosis, variation of muscle fibre diameters, increase in small fibres and collagen-containing tissue (blue in Masson Trichrome staining), are reduced in dy^W/mag and dy^W/Bcl/mag mice but are similar or stronger in dy^W/Bcl mice.

C. Percentage of fibrotic area per *triceps* cross-section. Mini-agrin reduces ($p = 0.007$), whereas Bcl2 increases ($p = 0.03$) fibrosis in dy^W/dy^W muscle. Fibrosis is comparable in dy^W/mag and dy^W/Bcl/mag muscles at 12- ($p = 0.22$) and at 16- ($p = 0.14$) weeks of age. $N \geq 3 \leq 5$.

D. Muscle fibre size distribution of 12-week-old mice. Values represent relative numbers of fibres in a given diameter class (5 μm/class). Dy^W/Bcl muscles contain many more small fibres than dy^W/dy^W muscles. The fibre size distribution of dy^W/Bcl/mag is shifted to smaller fibres compared to dy^W/mag or control (ctrl) muscles; $N = 4$.

E. Change in fibre size distribution from 12- to 16-week-old dy^W/Bcl/mag and dy^W/mag mice. Percentage of fibres with larger diameters increases from 12 to 16 weeks of age in dy^W/Bcl/mag (arrows) but not in dy^W/mag mice; $N = 4$.

F. Mean fibre diameter. The size of dy^W/Bcl/mag fibres increases from 12 to 16 weeks of age (two-way ANOVA: $p = 0.02$) and becomes similar to the mean fibre size in dy^W/mag muscle ($p = 0.22$); $N = 4$.

G. Muscle area (mm^2) of mid-belly *triceps* cross-sections. Control muscle has nearly twice the size compared to all the other genotypes at 12 weeks of age. Although not significantly different over all time points (two-way ANOVA: $p = 0.058$), muscle area of dy^W/Bcl/mag mice increases from 12 to 16 weeks of age (two-way ANOVA: $p = 0.026$) and becomes significantly larger than in dy^W/mag mice ($p = 0.03$) at 16 weeks of age; $N = 4$.

H. Total number of fibres per *triceps* cross-section. At 12 weeks of age, dy^W/dy^W ($p < 0.001$) and dy^W/mag ($p = 0.001$) muscles have a significantly reduced number of fibres, whereas, the fibre number is near normal in dy^W/Bcl ($p = 0.8$) and dy^W/Bcl/mag ($p = 0.08$) mice. In 16-week-old dy^W/Bcl/mag mice, the number of fibres is similar to controls ($p = 0.86$). Two-way ANOVA analysis confirmed the normalization of the fibre number over all ages in dy^W/Bcl/mag when compared to dy^W/mag muscle ($p < 0.0001$). Bcl2 expression did not increase the number of fibres on WT background (Bcl); $N \geq 3 \leq 5$. All values represent the mean ± SEM; *N* indicates the animal number per experimental group. *p*-Values are Student's *t*-test ($^{***}p \leq 0.001$; $^{**}p \leq 0.01$; $^{*}p \leq 0.05$; n.s. $p > 0.05$) or two-way ANOVA if indicated ($^{\circ}p \leq 0.05$). Size bars = 100 μm.

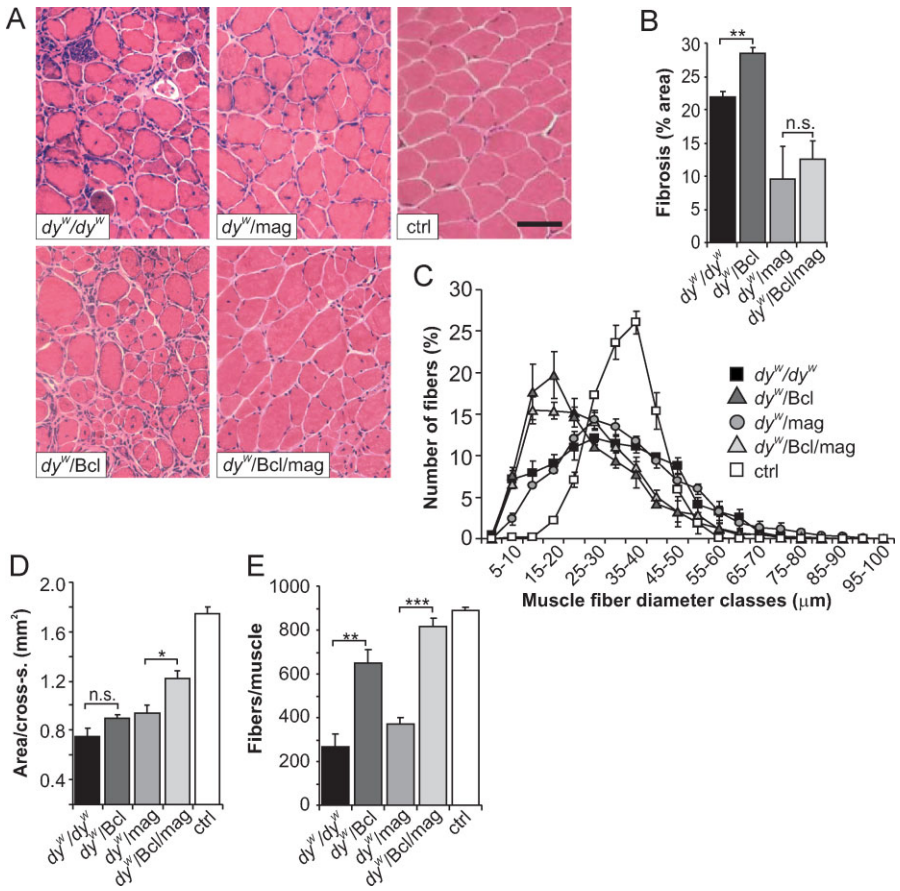

Figure 2. Histological analysis of *soleus* muscle from 12-week-old mice.

A. H & E staining of *soleus* cross-sections. Whereas, mini-agrin reduces fibrosis (dy^W/mag and dy^W/Bcl/mag), small fibres are very frequent in dy^W/Bcl muscle.

B. Percentage of fibrotic area in *soleus* cross-sections. Fibrosis is more prominent in dy^W/Bcl than in dy^W/dy^W ($p = 0.002$) muscle. In dy^W/mag and dy^W/Bcl/mag mice, fibrosis is similar ($p = 0.49$) and is lower compared to dy^W/dy^W muscle (dy^W/mag: $p = 0.004$; dy^W/Bcl/mag: $p = 0.005$); $N \geq 3 \leq 4$.

C. Muscle fibre size distribution. Values represent relative numbers of fibres in a given diameter class (5 μm/class). None of the transgenes was able to normalize the fibre size distribution; $N = 4$.

D. Muscle area (mm^2) of mid-belly *soleus* cross-sections. Area is increased in dy^W/Bcl/mag muscle compared to dy^W/mag ($p = 0.014$) muscle; $N \geq 3 \leq 4$.

E. Total number of fibres per *soleus* cross-section. The number of fibres is increased in dy^W/Bcl and dy^W/Bcl/mag mice compared to dy^W/dy^W and dy^W/mag mice. The number of fibres in dy^W/Bcl/mag mice reaches that found in WT controls, whereas, mini-agrin alone does not strongly influence fibre numbers; $N \geq 3 \leq 4$. *N* indicates the animal number per experimental group. $p > 0.05$). Size bars = 100 μm.

the fibrosis, inflammation was reduced by the co-expression of mini-agrin. The same histological results were also obtained in the *soleus* muscle of 12-week-old mice (Fig 2A and B and Fig S2B of Supporting information), indicating that the progressed paralysis of the hindlegs did not affect fibrosis.

As respiratory insufficiency is one of the clinical symptoms of MDC1A patients, we also examined the general histopathology of the diaphragm by H & E staining (Fig S3A of Supporting information) and measured fibrosis using the hydroxyproline assay (Fig S3B of Supporting information). The diaphragm of 12-week-old dy^W/dy^W mice was thin, fibrotic and showed a clearly reduced fibre number per width when compared to the other genotypes. Fibrosis was also prominent in the diaphragm of dy^W/Bcl mice. In dy^W/mag and dy^W/Bcl/mag mice, the diaphragms were wider and less fibrotic. Moreover, the phenotype did not significantly worsen between the age of 12 and 16 weeks (Fig S3A and B of Supporting information). These results are largely the same as those obtained in *triceps brachii* and *soleus* muscles.

Combined treatment with mini-agrin and Bcl2 enables the dy^W/dy^W muscle to grow

Change in muscle fibre size distribution is a hallmark of MDC1A and dy^W/dy^W mice. Expression of Bcl2 increased the number of small fibres even further, both in *triceps* (Fig 1D) and *soleus* (Fig 2C), whereas, expression of mini-agrin normalized the fibre size distribution. Interestingly, co-expression of mini-agrin with Bcl2 reversed the effect of Bcl2 alone and resulted in the normalization of fibre size distribution in 16-week-old mice, reaching the same profile as seen in dy^W/mag mice (Fig 1E and

F). This normalization was also seen in the mean size of muscle fibres (Fig 1F). In contrast to *triceps* muscle, no effect of mini-agrin on muscle fibre size distribution was observed in *soleus* muscle (Fig 2C). Because mini-agrin and Bcl2 are not expressed in peripheral nerve (Dominov et al, 2005; Moll et al, 2001), the paralysis of the hindlegs was not prevented at this age. Thus, the small fibre size in transgenic mice is probably due to the atrophy induced by the paralysis of the hindlegs.

During our analysis, we realized that the total area of mid-belly cross-sections of *triceps* (Fig 1G) and *soleus* (Fig 2D) muscle from 12-week-old dy^W/dy^W mice was much smaller than in age-matched controls. Overexpression of Bcl2, mini-agrin or the combination of both caused a small but non-significant increase in the cross-sectional area (CSA; Fig 1G and Fig 2D). Interestingly, when mini-agrin was co-expressed with Bcl2, this trend to increase the CSA became significant in *triceps* muscle from 16-week-old mice (Fig 1G). Because of the peripheral neuropathy that causes a progressive atrophy of the hindleg muscles in dy^W/dy^W (Miyagoe-Suzuki et al, 2000) as well as in dy^W/Bcl, dy^W/mag and dy^W/Bcl/mag mice, this effect was not examined in *soleus* muscles from 16-week-old mice. However, the results obtained from *triceps* indicate that muscle of dy^W/Bcl/mag mice has the capability to grow.

Bcl2 enables the maintenance of the original muscle fibre number in dy^W/dy^W mice

Next, we tested whether the change in muscle area was due to changes in the total number of muscle fibres. While 12-week-old dy^W/dy^W and dy^W/mag mice contained about 40% fewer fibres than controls (Fig 1H and 2E), the number of fibres was largely normalized in dy^W/Bcl and dy^W/Bcl/mag mice, both in the *triceps* (Fig 1H) and *soleus* muscle (Fig 2E). Moreover, the number of fibres remained normal in the *triceps* of 16-week-old dy^W/Bcl/mag mice. Interestingly, Bcl2 expression on a wild-type (WT) background (Bcl) did not increase the fibre number (Fig 1H), suggesting that Bcl2-mediated inhibition of apoptosis may allow the dy^W/dy^W muscle to maintain the original fibre number, including the small fibres that would have disappeared in the absence of Bcl2.

To verify the role of apoptosis in the loss of fibres in dy^W/dy^W mice, we used TdT-mediated dUTP nick end labelling (TUNEL) which recognizes nuclear *in situ* DNA-strand breaks that occur in nuclei undergoing apoptosis. In dy^W/dy^W and dy^W/mag muscles, apoptotic TUNEL-positive muscle fibres could be identified (Fig 3A, arrows) and represented 1.7 and 1% of all fibres, respectively (Fig 3B). In contrast, no TUNEL-positive myonuclei were found upon Bcl2 expression. The TUNEL-positive nuclei detected in dy^W/Bcl and dy^W/Bcl/mag mice all seemed to belong to non-muscle cells (Fig 3A, arrowheads). Apoptosis has been suggested to increase during abortive muscle regeneration in MDC1A patients (Hayashi et al, 2001) and mouse models thereof (Bentzinger et al, 2005; Dominov et al, 2005; Girgenrath et al, 2004; Kuang et al, 1999). To account for this, we also counted the number of TUNEL-positive, centrally localized myonuclei. Central nucleation has been shown to be indicative of regenerative processes. As shown in Fig 3C, *triceps* muscle from dy^W/dy^W and dy^W/mag contained more regenerating fibres that were TUNEL-positive than those expressing Bcl2. These results indicate that Bcl2 largely prevents the death of fibres both in normal and regenerating muscle, which may maintain the number of fibres to the levels of control mice.

Bcl2 enhances the regeneration efficiency in dy^W/mag muscle

Besides its function in stabilizing muscle fibres during contraction, LM-211 has also been shown to be important for the successful regeneration of muscle (Bentzinger et al, 2005; Kuang et al, 1999). In addition, regeneration is improved in dy^W/mag mice (Meinen et al, 2007). Regenerating muscle fibres transiently express the developmental form of myosin heavy chain (dMyHC; Novocastra, NCL-MHCd) and newly regenerated fibres have their nuclei in the centre and not in the periphery. Thus, the number of dMyHC-positive and centrally nucleated fibres (CNF) is a measure of ongoing and successful regeneration. To assess the role of apoptosis inhibition in the regeneration process, we first counted the number of CNF in the different mouse models. As shown earlier, the number of CNF was increased in dy^W/dy^W mice due to ongoing muscle degeneration when compared to WT controls (Fig 4A). Expression of Bcl2 resulted in a further threefold increase in the number of CNF, suggesting that regeneration of muscle fibres is more effective. Similarly, the number of CNF was increased in dy^W/mag mice compared to dy^W/dy^W but was lower than in dy^W/Bcl mice. This finding is consistent with the previous interpretation that mini-agrin enables successful regeneration but primarily prevents muscle degeneration by its linking of the basement membrane to α-dystroglycan (Moll et al, 2001). Interestingly, expression of both Bcl2 and mini-agrin resulted in a further increase of the number of CNF in 12- and 16-week-old mice compared to dy^W/mag mice. To test for ongoing regeneration, we also stained for dMyHC. As with CNF, the number of dMyHC-positive fibres in *triceps* muscle was several fold higher in dy^W/Bcl than in dy^W/dy^W mice and the effect of Bcl2 was also seen when combined with mini-agrin (Fig 4B and C).

To follow muscle regeneration directly, we next injected the myotoxin notexin into *tibialis anterior* muscle and examined muscles over time. One week post-injection, regenerating dMyHC-expressing fibres were rare and small in dy^W/dy^W muscle while many fibres were dMyHC-positive in all the other genotypes (Fig 4D). Strikingly, the regenerating fibres in dy^W/Bcl mice were very small and the muscle included large regions with mononucleated cells and damaged tissue (Fig 4D, asterisks). In contrast, regenerating fibres in dy^W/mag and dy^W/Bcl/mag mice were rather large and reached a similar size as in controls. Two weeks after notexin injection, the structure of the entire muscle was re-built in dy^W/mag, dy^W/Bcl/mag and control muscles, whereas, the muscle in dy^W/Bcl and dy^W/dy^W mice contained large fibrotic regions (asterisks) and the fibres remained unconnected (Fig 4E and F). Thus, although the muscle of dy^W/Bcl mice shows early signs of a successful regeneration, late steps in this process are not completed. In contrast, these late steps are successfully completed if mice are also transgenic for mini-agrin.

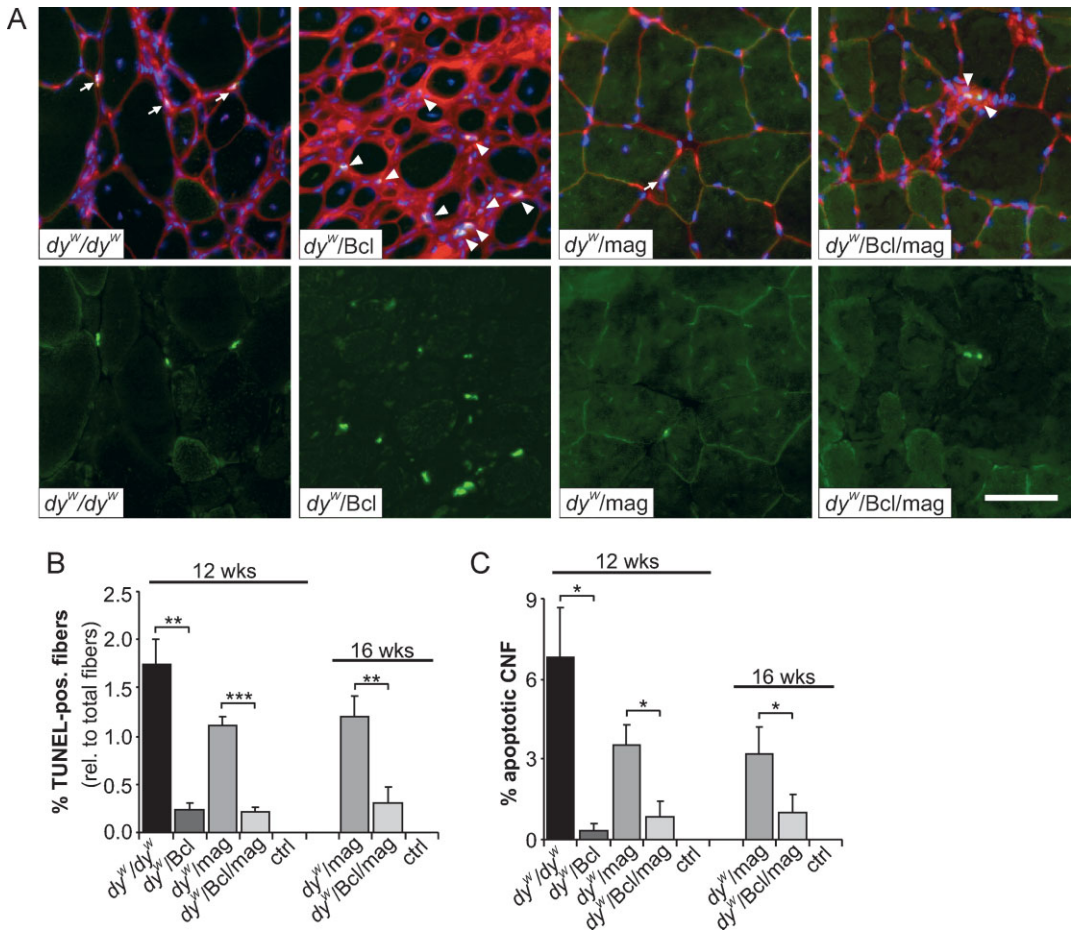

Figure 3. Apoptosis in *triceps brachii*.

A. Apoptotic nuclei recognized by TUNEL staining (green, separately shown in the bottom row) of *triceps brachii* cross-sections from 12-week-old mice. Muscles were counterstained with WGA (red) to visualize membranes and fibrotic areas and with DAPI (blue) to stain nuclei. Muscle fibres containing apoptotic nuclei are found in dy^W/dy^W and to a lower extent in dy^W/mag muscle (arrows). Apoptotic nuclei recognized in dy^W/Bcl and dy^W/Bcl/mag muscle reside outside of the muscle fibres (arrowheads).

B. Relative number of the TUNEL-positive muscle fibres. Bcl2 expression inhibits apoptosis in muscle fibres of dy^W/dy^W ($p = 0.004$). Similarly, Bcl2 prevents apoptosis in dy^W/mag mice at 12 weeks ($p \leq 0.001$), at 16 weeks ($p = 0.002$) as well as over both ages (two-way ANOVA: $p < 0.0001$); $N \geq 3 \leq 4$.

C. Percentage of centrally localized nuclei that undergo apoptosis. In dy^W/dy^W muscles almost 7% and in dy^W/mag muscles 3.5% of the regenerating fibres are TUNEL-positive. Apoptosis of regenerating fibres is strongly decreased by expression of Bcl2 in muscles of dy^W/dy^W ($p = 0.02$) and dy^W/mag mice (12 weeks: $p = 0.03$; 16 weeks: $p = 0.04$; two-way ANOVA over both ages: $p = 0.0027$); $N \geq 3 \leq 4$. All values represent the mean ± SEM; N indicates the animal number per experimental group. p-Values are Student's t-test ($^{***}p \leq 0.001$; $^{**}p \leq 0.01$; $^{*}p \leq 0.05$; n.s. $p > 0.05$) or two-way ANOVA as noted above. Size bars = 50 μm.

Effect of co-expression of Bcl2 and mini-agrin on behaviour and survival in dy^W/dy^W mice

We next evaluated the effect of the different treatments on overall health. As a single transgene, Bcl2 had a moderate but significant effect on survival, whereas, mini-agrin tripled mean survival compared to dy^W/dy^W mice (Fig 5A). Although mice that expressed both mini-agrin and Bcl2 survived a little bit longer than dy^W/mag mice, the difference was not significant. Bcl2 had also a small effect on body weight (Fig 5B), overall health (Fig 5C), locomotory activity (Fig 5D) and grip strength (Fig 5E). Compared to dy^W/dy^W mice, the effect of Bcl2 was significant over all time points (see figure legend). Transgenic expression of Bcl2 was also beneficial in dy^W/mag mice in all those paradigms and the effect was significant over all time points for the body weight (Fig 5B) and the grip strength (Fig 5E) but not for the locomotion (Fig 5D). Interestingly though, locomotion reached significance at the last time point of 16 weeks (compare dy^W/Bcl/mag with dy^W/mag). Thus, these data confirm previous work using Bcl2 (Dominov et al, 2005; Girgenrath et al, 2004) but also show that the effect of mini-agrin is much larger than that of Bcl2 and that the additional benefit gained by co-expressing Bcl2 with mini-agrin is rather small and becomes significant at the older age.

Muscle function is improved in dy^W/Bcl/mag mice

To test directly whether the difference on grip strength reflected an improvement in the force of muscles, we next measured the contractile properties in isolated *extensor digitorum longus*

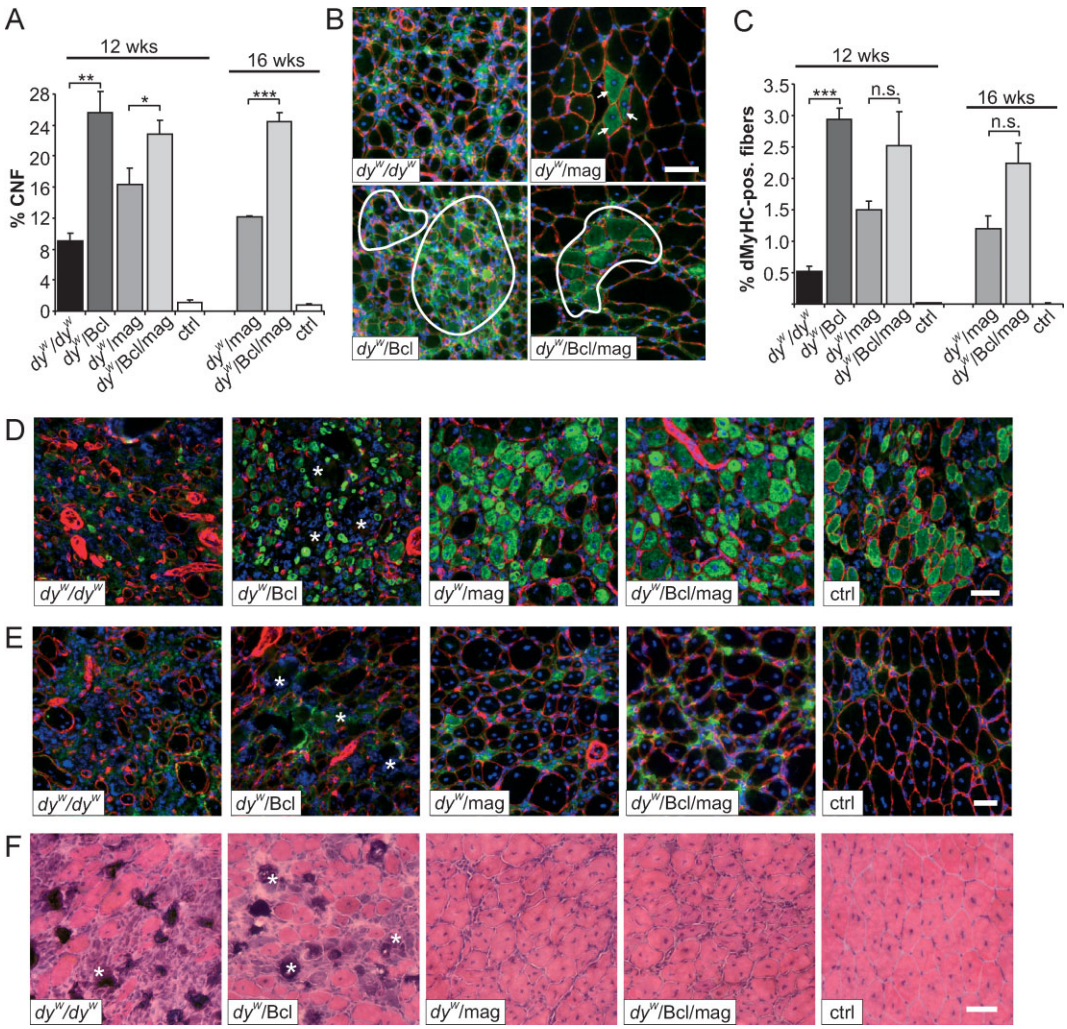

Figure 4. Spontaneous and injury-induced muscle regeneration.

A. Percentage of CNF. In dy^W/dy^W mice, only 9% of the muscle fibres are centrally nucleated, indicative of impaired regeneration. In dy^W/mag muscle the number of CNF is increased and is further elevated by co-expression of Bcl2 in both 12- and 16-week-old dy^W/Bcl/mag mice (two-way ANOVA over all ages: $p < 0.0001$); $N = 4$.

B. Spontaneous muscle regeneration in 12-week-old muscles. Antibodies to dMyHC (green) and laminin-γ1 (red) were used. DAPI (blue) visualizes nuclei. Only few dMyHC-positive fibres are found in dy^W/dy^W mice. Some more dMyHC-positive fibres are present in dy^W/mag (arrows) muscle, whereas, many more are detected upon Bcl2 expression in dy^W/Bcl and dy^W/Bcl/mag (encircled areas).

C. Quantification of dMyHC-positive fibres. The number of dMyHC-positive fibres is highest in Bcl2 transgenic mice (dy^W/Bcl and dy^W/Bcl/mag) followed by dy^W/mag and dy^W/dy^W mice. Although not significant at 12 or 16 weeks of age (*t*-test), the increase of dMyHC-positive fibres in dy^W/Bcl/mag compared to dy^W/mag muscles becomes significant when measured over all ages (two-way ANOVA: $p = 0.022$). No spontaneous regeneration was detected in control muscles (ctrl); $N \geq 4 \leq 6$.

D.–F. Regenerative response of *tibialis anterior* muscle of 6-week-old mice after notexin injection.

D. Muscle cross-sections were stained with antibodies to dMyHC (green) and laminin-γ1 (red), and with the nuclear marker DAPI (blue) 1 week after notexin injection. Only very few dMyHC-positive fibres are detected in dy^W/dy^W mice, while many muscle fibres are dMyHC-positive in dy^W/Bcl, dy^W/mag, dy^W/Bcl/mag and control (ctrl) mice. Note that muscle fibres in dy^W/Bcl mice are small; $N \geq 4 \leq 5$.

E. Regeneration status of *tibialis anterior* 2 weeks after notexin injection. Antibodies to dMyHC (green), laminin-γ1 (red) and the nuclear marker DAPI (blue) were used. Absence of dMyHC-positive fibres and large areas devoid of laminin-γ1 staining (asterisks) are indicators of the failed regeneration in dy^W/dy^W and dy^W/Bcl muscles. The presence of few dMyHC-positive fibres and the non-disrupted laminin-γ1 staining indicate successful muscle regeneration in dy^W/mag, dy^W/Bcl/mag and control mice; $N \geq 3 \leq 4$.

F. H & E staining of *tibialis anterior* 2 weeks after notexin injection shows the failure in regeneration leading to fibrosis in dy^W/dy^W and dy^W/Bcl muscles (asterisks) and the successful regeneration in dy^W/mag, dy^W/Bcl/mag and control mice; $N \geq 3 \leq 4$. All values represent the mean ± SEM; *N* indicates the animal number per each experimental group. *p*-Values are Student's *t*-test ($^{***}p \leq 0.001$; $^{**}p \leq 0.01$; $^{*}p \leq 0.05$; n.s. $p > 0.05$) or two-way ANOVA as noted in the text. Size bars = 50 μm.

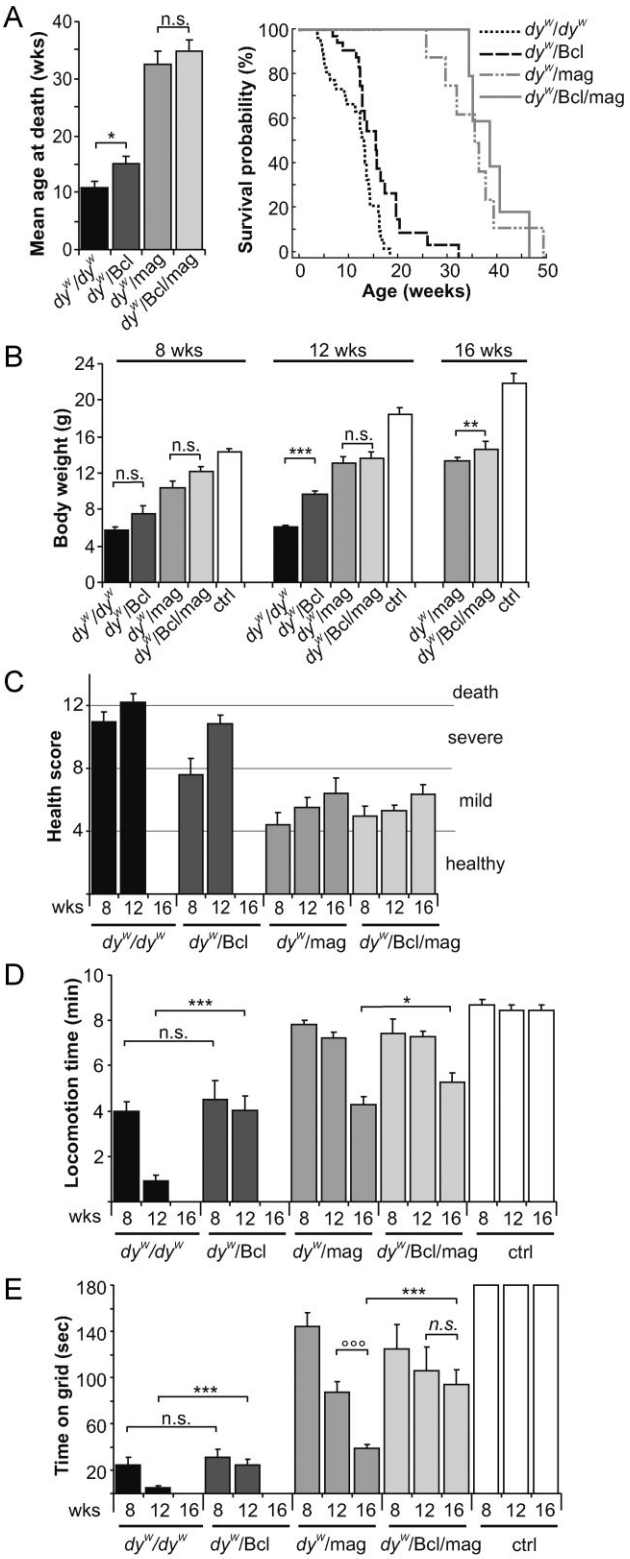

Figure 5. Survival and behaviour of mice.

A. Average survival (left panel) and Kaplan–Meier cumulative survival plot (right panel). Average survival of dy^W/dy^W mice increases by 30% upon Bcl2 expression ($p = 0.02$). Expression of mini-agrin triples the mean survival time ($p \leq 0.001$). In the few ($N = 5$) double transgenic dy^W/Bcl/mag mice tested, the survival was not prolonged compared to dy^W/mag mice; $N = 35$, 22, 8 and 5 for dy^W/dy^W, dy^W/Bcl, dy^W/mag and dy^W/Bcl/mag, respectively.

B. Body weight at the ages of 8, 12 and 16 weeks. Both transgenes increase the body weight of dy^W/dy^W mice. Although the effect of Bcl2 is rather small in comparison to the effect exerted by mini-agrin, Bcl2 significantly elevates body weight in dy^W/dy^W mice over all time points (two-way ANOVA: $p < 0.0001$). In addition, Bcl2 expression increases body weight over all ages in dy^W/mag mice (two-way ANOVA: $p = 0.002$); $N \geq 4 \leq 11$.

C. Overall health status of mice was judged by the assessment of activity, appetite, posture, fur and eyes of 8, 12 and 16-week-old mice. For details on the score sheet used see Materials and Methods Section; $N \geq 4 \leq 11$.

D. Open-field locomotion during 10 min. Bcl2 expression delays the loss of locomotory activity in dy^W/dy^W mice over all time points (two-way ANOVA: $p \leq 0.001$) but does not reach the same efficacy as mini-agrin. Although not significant over all time points (two-way ANOVA: $p = 0.28$), locomotion becomes improved in 16-week-old dy^W/Bcl/mag when compared to dy^W/mag mice ($p = 0.048$); $N \geq 4 \leq 11$.

E. Grip strength was measured by placing the mice on a vertical grid. The test was stopped after 180 s. Dy^W/Bcl mice are stronger than dy^W/dy^W mice measured over all time points (two-way ANOVA: $p = 0.005$). In 16-week-old dy^W/mag mice, co-expression of Bcl2 prevents the loss of grip strength ($p \leq 0.001$). Over all time points, Bcl2 increased the muscle strength of dy^W/mag mice (two-way ANOVA: $p = 0.014$); $N \geq 4 \leq 11$. All values represent the mean ± SEM; N indicates the animal number per experimental group; p-values are Student's t-test (***$p \leq 0.001$; **$p \leq 0.01$; *$p \leq 0.05$; n.s. $p > 0.05$) or two-way ANOVA if indicated (°°°$p \leq 0.001$; °°$p \leq 0.01$; °$p \leq 0.05$; *n.s.* $p > 0.05$).

(EDL; Table 1, Fig 6A, C and E) and *soleus* (Table 1; Fig 6B, D and F) muscles. To avoid falsification of the results by the MDC1A-typical progressing hindleg paralysis (Miyagoe-Suzuki et al, 2000), we analysed the muscles in young, 4-week-old animals, when paralysis was not yet prominent and muscle histology of dy^W/mag mice was still largely indistinguishable from control mice (Fig S4 of Supporting information). In both muscles, the wet weight, optimal contraction length (L_0), CSA and the twitch-to-tetanus ratio (P_t/P_0) increased from dy^W/dy^W, dy^W/Bcl, dy^W/mag and dy^W/Bcl/mag to control mice (Table 1). There was some improvement in most of the parameters from dy^W/dy^W to dy^W/Bcl mice, although this trend was never statistically significant (Table 1 and Fig 6). Interestingly, when Bcl2 and mini-agrin were co-expressed (dy^W/Bcl/mag) there was a significant increase in the absolute twitch force (P_t) compared to dy^W/mag mice in both EDL and *soleus* muscle (Table 1 and Fig 6A and B). Similarly, the normalized, maximum isometric tetanic force (P_o) was higher in dy^W/Bcl/mag mice than in dy^W/mag mice (Fig 6C and D). However, upon normalization of P_o to muscle size [i.e. maximum specific tetanic force (sP_o)], the significance of the difference between dy^W/mag and dy^W/Bcl/mag mice got lost (Fig 6E and F). The fact that the difference between dy^W/Bcl/mag and dy^W/mag mice is higher for the absolute force than the specific force is in agreement with our finding (Fig 1H and E)

Table 1. *In vitro* function of EDL and *soleus* muscles.

	dy^W/dy^W	dy^W/Bcl	dy^W/mag	dy^W/Bcl/mag	ctrl
Body weight (g)	8.4 ± 1.4	9.1 ± 1.2	14.3 ± 0.1	15.9 ± 1.1	21.3 ± 1.6
EDL					
$N_{muscles}$	6	5	5	7	6
Wet muscle mass (mg)	3.5 ± 0.5	3.8 ± 0.3	6.3 ± 0.8	6.7 ± 0.2	9.0 ± 0.4
L_0 (mm)	7.9 ± 0.3	8.4 ± 0.7	10.4 ± 0.2	10.4 ± 0.3	10.9 ± 0.4
CSA (mm^2)	0.42 ± 0.04	0.42 ± 0.01	0.54 ± 0.04	0.62 ± 0.04	0.78 ± 0.04
P_t (mN)	2.9 ± 1.5	4.3 ± 1.4	11.9 ± 1.7	24.6 ± 4.6	51.5 ± 5.3
sP_t (mN/mm^2)	5.9 ± 2.2	10.0 ± 3.2	20.5 ± 1.8	38.7 ± 6.7	67.5 ± 8.3
TP_t (ms)	12.0 ± 0.7	11.0 ± 0.4	10.8 ± 0.6	12.3 ± 0.9	12.5 ± 0.7
$RT_1/_2$ (ms)	37.4 ± 4.2	34.2 ± 3.5	30.9 ± 2.8	28.9 ± 0.9	30.8 ± 2.9
P_0 (mN)	20.9 ± 8.0	30.9 ± 5.3	84.2 ± 5.3	120.2 ± 11.0	227.5 ± 21.1
sP_0 (mN/mm^2)	42.3 ± 8.4	72.5 ± 11.8	146.2 ± 15.0	193.2 ± 24.4	297.2 ± 32.9
P_t/P_0	0.118 ± 0.02	0.129 ± 0.03	0.146 ± 0.02	0.195 ± 0.02	0.228 ± 0.02
soleus					
$N_{muscles}$	5	5	6	6	5
Wet muscle mass (mg)	3.46 ± 0.7	3.6 ± 0.3	3.8 ± 0.2	4.8 ± 0.2	7.3 ± 0.3
L_0 (mm)	8.0 ± 0.2	7.9 ± 0.3	8.25 ± 0.2	8.75 ± 0.3	9.1 ± 0.2
CSA (mm^2)	0.41 ± 0.08	0.42 ± 0.03	0.431 ± 0.03	0.52 ± 0.02	0.76 ± 0.03
P_t (mN)	1.8 ± 0.6	3.3 ± 0.6	5.4 ± 1.2	9.7 ± 1.3	21.6 ± 3.5
sP_t (mN/mm^2)	3.9 ± 0.8	7.6 ± 1.2	12.0 ± 2.2	20.7 ± 3.3	24.6 ± 2.6
TP_t (ms)	24.0 ± 0.9	26.4 ± 2.5	29.0 ± 2.0	24.0 ± 1.0	23.8 ± 1.7
$RT_1/_2$ (ms)	56.4 ± 4.0	59.2 ± 4.8	62.8 ± 3.5	57.4 ± 2.4	56.8 ± 5.3
P_0 (mN)	22.2 ± 7.9	30.4 ± 4.1	45.5 ± 8.5	70.2 ± 5.5	105.2 ± 14.6
sP_0 (mN/mm^2)	47 ± 13	71 ± 8	102 ± 14	124 ± 11	138 ± 17
P_t/P_0	0.092 ± 0.01	0.112 ± 0.02	0.115 ± 0.00	0.155 ± 0.03	0.164 ± 0.04

The table shows the *in vitro* contractile properties at 30°C of EDL and *soleus* muscle. Data (mean ± SEM) include: number of tested muscles ($N_{(muscles)}$), animal body weight (g), wet muscle weight (mg), optimal muscle length (L_0, mm), CSA (mm^2), peak twitch force (P_t; mN), specific twitch force represents P_t normalized to CSA (sP_t; mN/mm^2), time to peak twitch tension (TP_t; ms), half-relaxation time ($RT_1/_2$; ms), maximum isometric tetanic force (P_0; mN), maximum specific tetanic force (sP_0; mN/mm^2) and twitch tetanus ratio (P_t/P_0).

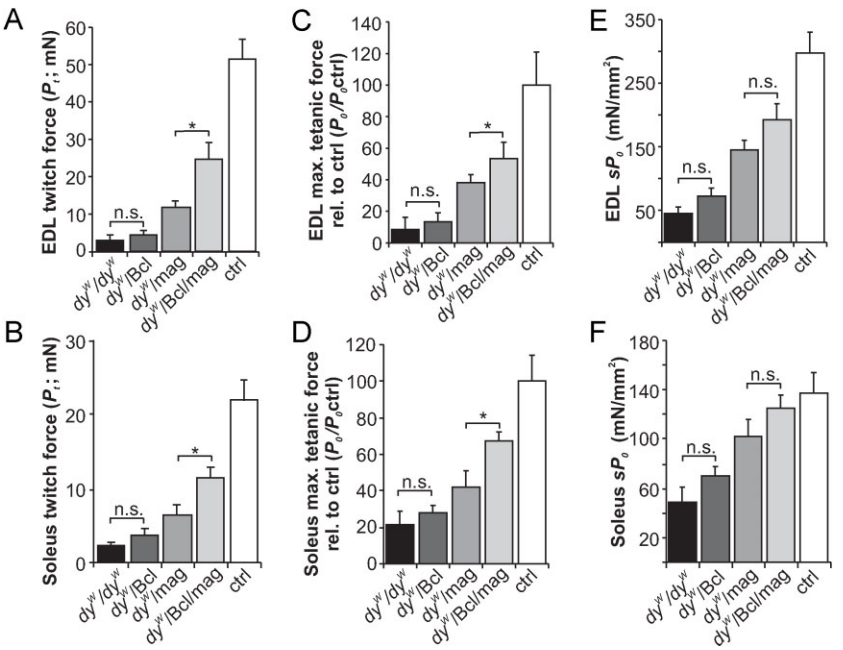

Figure 6. Contraction properties of EDL and *soleus* muscle.

EDL (**A, C, E**) and *soleus* (**B, D, F**) muscles from mice with the indicated genotypes.

A,B. Absolute twitch force (P_t), measured by a single electrical stimulation at 15 V, is similar in dy^W/dy^W and dy^W/Bcl mice (EDL: $p = 0.52$; *soleus*: $p = 0.15$) but increases from dy^W/Bcl to dy^W/mag (EDL: $p = 0.009$; *soleus*: $p = 0.05$), from dy^W/mag to dy^W/Bcl/mag (EDL: $p = 0.018$; *soleus*: $p = 0.03$) and from dy^W/Bcl/mag to control (EDL: $p = 0.006$; *soleus*: $p = 0.001$).

C,D. Maximum isometric tetanic force (P_0) of EDL (C) or *soleus* muscle (D) expressed as percentage of controls (P_0/P_0 ctrl). Co-expression of Bcl2 (dy^W/Bcl/mag) increases the maximal tetanic force of dy^W/mag in EDL ($p = 0.03$) and in *soleus* ($p = 0.02$).

E,F. The maximum specific tetanic force (sP_0) increases gradually from dy^W/dy^W to control mice in both EDL (E) and *soleus* (F). However, no significant change of sP_0 is seen between dy^W/Bcl/mag and dy^W/mag mice in EDL (E; $p = 0.07$) or in *soleus* (F; $p = 0.24$) muscle. All values represent the mean ± SEM; *N* numbers are shown in Table 1. *p*-values are Student's *t*-test ($^{***}p \leq 0.001$; $^{**}p \leq 0.01$; $^{*}p \leq 0.05$; n.s. $p > 0.05$).

that the number of fibres is much increased in dy^W/Bcl/mag mice. Thus, although the force generated per muscle fibre is not much higher in dy^W/Bcl/mag mice than in dy^W/mag mice, the total force is significantly increased. These data show that expression of Bcl2 in dy^W/mag mice increases muscle force by up to 50% and thus indicates that dy^W/dy^W mice do benefit from a combined treatment with mini-agrin and inhibition of apoptosis.

Pharmacological inhibition of apoptosis enhances amelioration by mini-agrin

We have recently shown that oral application of the pharmacological apoptosis inhibitor omigapil to dy^W/dy^W mice ameliorates MDC1A pathology (Erb et al, 2009). Based on the finding that transgenic expression of Bcl2 increased the therapeutic effect of mini-agrin, we next tested whether the combination of mini-agrin and systemic application of omigapil would be of benefit. To this end, dy^W/mag mice were treated with a daily dose of 0.1 mg/kg omigapil starting at the age of 15 days. The first week of treatment, omigapil was injected into the peritoneum followed by oral gavage after weaning. Mice were analysed at the age of 12 weeks. Visual inspection of H & E-stained cross-sections from *triceps* muscle did not reveal a striking difference between omigapil- (dy^W/mag-omigapil) and vehicle- (dy^W/mag-vehicle) treated dy^W/mag mice (Fig 7A). Quantitative assessment of changes showed, however, lowered creatine kinase (CK) levels in the blood (Fig 7B), normalized muscle fibre size distribution (Fig 7C), a trend to increasing the mean fibre size (Fig 7D) and to enlarging muscle area in dy^W/mag mice (Fig 7E). In addition, omigapil also reduced the muscle fibre loss in dy^W/mag mice (Fig 7F). Importantly, many of the functional parameters were significantly improved by omigapil. Those included body weight gain (Fig 7G), locomotive activity in the open-field test (Fig 7H) and grip strength (Fig 7I). However, we could not detect a difference in the overall survival (Fig 7J). Together, treatment of dy^W/mag mice with omigapil further improved several of the disease parameters but did not affect survival.

DISCUSSION

In this work, we tested whether the combination of anti-apoptosis treatment and transgenic expression of mini-agrin has additive effects on the disease progression in a mouse model for MDC1A. Indeed, we find such an additive effect for several of the parameters measured. This was particularly obvious in the grip strength (Fig 5E), the force measurements on isolated muscles (Fig 6), and the number and size of muscle fibres (Fig 1).

Combination of mini-agrin and Bcl2 improves force production in MDC1A muscles

Our data indicate that expression of Bcl2 is the key factor that preserves the number of muscle fibres while expression of mini-agrin is important for the preservation of force in individual muscle fibres. Support for this hypothesis stems from the singly transgenic mice. In dy^W/Bcl mice, the muscles contain the same number of fibres as in control mice (Fig 1E). However, the muscle fibres in dy^W/Bcl mice are small, even significantly smaller than those in dy^W/dy^W mice (Fig 1D and F). This decrease can explain the finding that the area of mid-belly cross-sections remains as small as in dy^W/dy^W muscles (Fig 1G) despite the increase in fibre number and fibrosis (Fig 1C; Fig S2A of Supporting information).

Thus, prevention of apoptosis by Bcl2 seems to allow survival but not the growth of muscle fibres. Mice singly transgenic for mini-agrin, in contrast, show a fibre size distribution that is close to that in control muscles (Fig 1D and E), but individual muscles of the dy^W/mag mice contain fewer fibres (Fig 1H). Consequently, the area of mid-belly cross-sections is still smaller than in control muscles (Fig 1G). Thus, mini-agrin seems to allow growth and stabilization of muscle fibres. Intriguingly, the combination of Bcl2 and mini-agrin increases the CSA in *triceps* muscle up to 70% of that of control muscle (Fig 1G). Importantly, co-expression of Bcl2 and mini-agrin tended to further potentiate the gain of muscle force measured *in vitro* (Fig 6). The fact that this test was performed in as young as 4-week-old mice, an age at which the typical hindleg paralysis of dy^W/dy^W mice is not yet prominent and at which muscle histology of dy^W/mag mice is comparable to control mice (Fig S4 of Supporting information; Moll et al, 2001), indicates that co-expression of the two transgenes indeed improves muscle strength and not only delays the loss of muscle force in dy^W/dy^W mice. Together, these results suggest that inhibition of apoptosis by Bcl2 in combination with the mechanical stabilization of muscle by mini-agrin can enhance contractile properties of muscle.

Mini-agrin and Bcl2 potentiate their effect on muscle regeneration in dy^W/dy^W mice

Besides the function of LM-211 to stabilize muscle fibre integrity, its binding to α7β1 integrin has been suggested to activate signals important for survival (Vachon et al, 1996, 1997). Muscle regeneration is strongly impaired in dy^W/dy^W and dy^{3K}/dy^{3K} mice (Bentzinger et al, 2005; Kuang et al, 1999; Miyagoe et al, 1997) and Bax levels have been shown to be increased during regeneration (Olive & Ferrer, 2000). Thus, non-productive muscle regeneration in laminin-α2-deficient mice might be due to increased apoptosis and inhibition of apoptosis may thus be particularly important during regenerative processes. Indeed, Bcl2 levels have been shown to be considerably increased in the early period of muscle fibre regeneration (Bulyakova & Azarova, 2006; Shefer et al, 2002).

When we tested this idea, we found that many muscle fibres of dy^W/Bcl mice contained centralized myonuclei and re-expressed the regeneration marker dMyHC (Fig 4B). One week after notexin-induced muscle damage, many muscle fibres of dy^W/Bcl mice were dMyHC-positive (Fig 4D) but regeneration was not successful after 2 weeks (Fig 4E and F) because most of the initially formed muscle fibres remained unconnected and were replaced by fibrotic tissue. Co-expression of mini-agrin prevented this fibrosis, allowed regenerating fibres to increase in diameter and to re-build a structured muscle tissue (Fig 4E and F). Thus, the combined treatment of apoptosis inhibition and mini-agrin expression increased the regeneration efficiency in dy^W/dy^W muscles. This effect is based on the Bcl2-mediated prevention of apoptosis at early stages of regeneration and the mini-agrin-

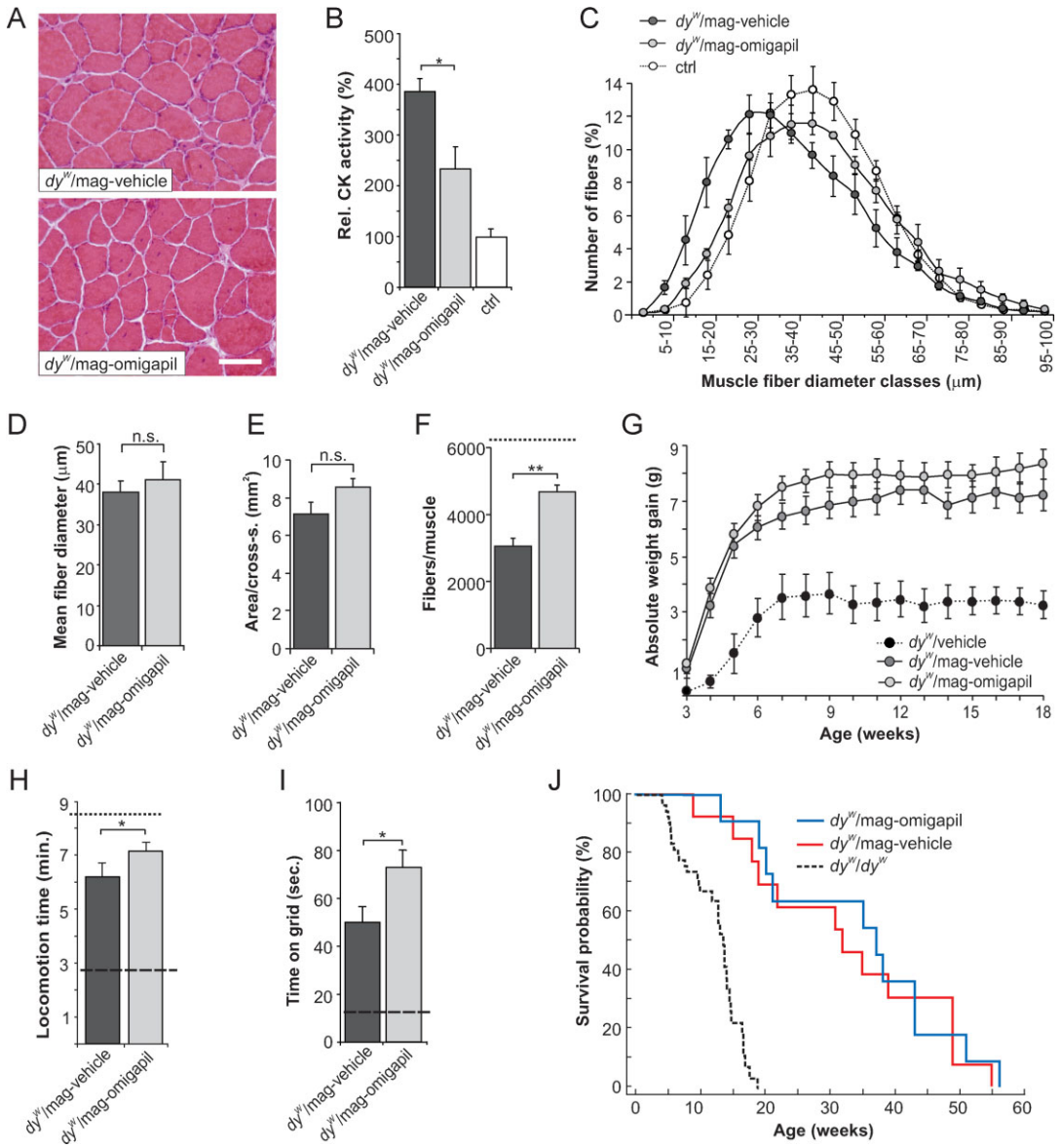

Figure 7. Effects of omigapil treatment in 12-week-old dy^W/mag mice.

A. H & E staining of cross-sections from *triceps brachii* muscle of dy^W/mag mice treated daily with 0.1 mg/kg omigapil (dy^W/mag-omigapil) or vehicle (dy^W/mag-vehicle).

B. Blood CK levels expressed as percentage of control. Omigapil treatment in dy^W/mag mice significantly lowers the CK levels ($p = 0.023$); $N \geq 6 \leq 8$.

C. Muscle fibre size distribution of *triceps brachii*. Values represent relative numbers of fibres in a given diameter class (5 μm/class). Muscles from vehicle-treated dy^W/mag mice contain more small-caliber fibres than muscles from age-matched dy^W/mag-omigapil mice; $N = 5$.

D. Mean fibre diameter. Omigapil treatment slightly but not significantly ($p = 0.07$) elevates the mean fibre size in dy^W/mag muscles; $N = 5$.

E. Muscle area (mm^2) of mid-belly *triceps* cross-sections. Omigapil treatment tends to enlarge muscle area in dy^W/mag mice ($p = 0.06$); $N = 5$.

F. Total number of fibres per *triceps* cross-section. Omigapil treatment reduces muscle fibre loss in dy^W/mag ($p = 0.006$) but does not completely normalize fibre numbers, as control muscle contain >6000 fibres (dashed line); $N = 5$.

G. Weight gain normalized to the body weight at 15 days of age (onset of treatment). For each week, body weight data were averaged from daily measurements. Body weight at 15 days of age (starting body weight) was 5.55 ± 0.20 g for dy^W/mag-omigapil mice and 6.88 ± 0.21 g for dy^W/mag-vehicle mice. Body weight curve for vehicle-treated dy^W/dy^W mice (Erb et al, 2009) is shown for comparison (dotted line); $N \geq 9 \leq 11$.

H. Locomotion within a 10 min observation period. Locomotive activity of dy^W/mag-omigapil mice is significantly increased compared to vehicle-treated dy^W/mag mice ($p = 0.046$). Locomotion of dy^W/dy^W (dashed line) and WT control mice (dotted line) are given for comparison; $N \geq 9 \leq 11$.

I. Grip strength is expressed as time mice were able to hold on a vertical grid. Omigapil treatment significantly increases the grip strength in dy^W/mag mice ($p = 0.02$). Grip strength of dy^W/dy^W mice is indicated (dashed line). WT control mice stay >180 s on the grid; $N \geq 9 \leq 11$.

J. Kaplan–Meier cumulative survival plot. Daily treatment (0.1 mg/kg) with omigapil does not improve the survival probability of dy^W/mag mice. All values are mean ± SEM. *N* indicates the animal number per experimental group. *p*-Values are Student's *t*-test ($^{***}p \leq 0.001$; $^{**}p \leq 0.01$; $^{*}p \leq 0.05$; n.s. $p > 0.05$). Scale bar = 50 μm.

mediated reconnection of the muscle fibres to the extracellular matrix, which is essential to complete regeneration. In addition and since notexin leaves the satellite cells unharmed, the added benefit by combining Bcl2 and mini-agrin in the muscle regeneration process might also originate, at least in part, from a protective effect on the satellite cells. Thus, the cumulative action of Bcl2 and mini-agrin during spontaneous muscle regeneration is probably the molecular basis for the overall increase in fibre number and size in the dy^W/Bcl/mag mice.

Systemic inhibition of apoptosis prevents the inflammatory phenotype of muscle-restricted Bcl2 expression

Mini-agrin is known to markedly reduce the replacement of muscle with fibrotic tissue. Unlike others (Dominov et al, 2005), we observed prominent fibrosis (Fig 1A–C; Fig 2A and B) and inflammation (Fig 2A and B of Supporting information) in muscles of dy^W/Bcl mice. Indeed, Bcl2 expression under control of the muscle-specific MyoD promoter inhibits apoptosis in dy^W/dy^W muscle fibres (Fig 3A and B), but accumulates other (inflammatory) cell types that frequently are apoptotic (Fig 3A, arrowheads). Together with the finding that Bcl2 impairs the removal of damaged tissue from notexin-injured dy^W/dy^W muscle (Fig 4D and E), the increased fibrosis in muscles of dy^W/Bcl mice may trigger an inflammatory response that activates macrophages. Although the mechanical muscle stabilization by mini-agrin largely counteracts this adverse effect of Bcl2 (Fig 1A–C; Fig 2A and B; Fig S2C and D of Supporting information), only a generalized inhibition of apoptosis can prevent the inflammatory response completely. This is seen in the experiments using oral application of omigapil (Erb et al, 2009) or in the whole-body deletion of the pro-apoptotic gene Bax (Girgenrath et al, 2004). Thus, the increased fibrosis in the Bcl2 transgenic mice might be due to the restricted inhibition of apoptosis to skeletal muscle.

In this context, we also noticed that omigapil already at 12 weeks of age enhanced the ameliorative effect of mini-agrin and improved fibre size distribution (Fig 7F), mean fibre size (Fig 7D), muscle area (Fig 7E), grip strength (Fig 7I) and locomotion (Fig 7H). In contrast, in dy^W/Bcl/mag mice these parameters were ameliorated only at the age of 16 weeks (Fig 1E–G; Fig 5D and E). It is well possible that this age-specific difference relies on the fact that inhibition of apoptosis by systemic application of omigapil acts on many cell types, whereas, inhibition of apoptosis by Bcl2 expression is restricted to muscles. Therefore, we think that the increased fibrosis and inflammatory phenotype upon muscle-restricted Bcl2 expression in dy^W/dy^W mice is a secondary effect that resides in another cell type than muscle fibres and thus might not be of concern for the treatment of MDC1A.

Translational aspects for the treatment of MDC1A by mini-agrin or apoptosis inhibitors

Another important insight of our studies is the observation that the efficacy of mini-agrin is by far greater than that of anti-apoptosis treatment. This is particularly striking in the survival, overall health, the locomotive activity and muscle force measurements (grip strength and force measurements on isolated muscle). For example, although Bcl2 expression or omigapil treatment extend the lifespan of dy^W/dy^W mice (Fig 5A; Dominov et al, 2005; Erb et al, 2009), no prolongation of lifespan was seen in the dy^W/Bcl/mag mice (Fig 5A). This lack of efficacy is probably due to the extended lifespan of dy^W/mag mice, which makes it difficult to detect a significant further increase by anti-apoptosis treatment. However, when the mice were forced to hold themselves on a vertical grid, dy^W/Bcl/mag mice could hold-on the grid more than twice as long as dy^W/mag mice (Fig 5E). Correspondingly, the orally administered anti-apoptotic drug omigapil also improved muscle strength in dy^W/mag mice (Fig 7I). The improvement of muscle function is of utmost importance for MDC1A patients.

We hypothesize that the difference in efficacy between mini-agrin and apoptosis inhibition is due to the different levels where the two treatments interfere with the disease process. While mini-agrin will take over at least some of the structural functions of LM-211, apoptosis is a late step in the cascade of events triggered by the absence of the laminin-α2 chain and thus its interference with the disease process is less specific. On the other hand, interference with such late steps has the advantage that potential drugs can be useful for a broad range of muscle dystrophies as those late events are common to several diseases. One possible mechanism underlying the additive effect of mini-agrin and the anti-apoptotic treatment could be the well-described effect of LM-211 to bind to α7β1 integrin. This interaction has been proposed to be important for the prevention of muscle fibre death (Vachon et al, 1996, 1997). As mini-agrin does not bind to this integrin, it can also not prevent apoptosis induced by the loss of LM-211 in dy^W/dy^W mice.

In conclusion, a combined treatment with apoptosis inhibitors and mini-agrin increases the regeneration efficiency in dy^W/dy^W muscles and, thereby, maintains muscle integrity. This in turn, enables the muscle to increase in size (Fig 1G and 2D), which results in the improvement of muscle strength and function (Fig 5D and E). Thus, a treatment that makes use of the additive benefit of apoptosis inhibition and mini-agrin might constitute a valuable therapy for MDC1A patients. However, realization of a combined treatment involves the development of a method that delivers mini-agrin to the skeletal muscles of human MDC1A patients, which is not feasible at the moment. Thus, pharmacological treatment options can probably be developed much faster. This is particularly true for omigapil, which shows the same efficacy as transgenic expression of Bcl2 (this work). Its clinical development is well advanced and it was proven to be safe in large clinical trials with Parkinson's disease and amyotrophic lateral sclerosis patients (Miller et al, 2007; Olanow et al, 2006).

MATERIALS AND METHODS

Mice

Dy^W/dy^W mice containing a LacZ insertion in the *LAMA2* gene served as the mouse model for MDC1A. Genotyping of dy^W/dy^W mice was performed as previously described (Kuang et al, 1998a). The chick mini-agrin transgene (mag) was expressed under the control of the muscle-specific CK promoter (Moll et al, 2001). The mice were genotyped as described (Meinen et al, 2007). Transgenic mice expressing full-length

human Bcl2 under control of an approximately 7 kb-long fragment of the mouse MyoD promoter (Dominov et al, 2005; Girgenrath et al, 2004; Tapscott et al, 1992) were obtained from Dr Janice Dominov. The MyoD promoter was described to be active in myoblasts, activated satellite cells and in muscle fibres (Charge et al, 2008; Dominov et al, 2005; Girgenrath et al, 2004; Tapscott et al, 1992). Since their generation, all of the transgenic mouse lines were maintained in C57BL/6J mice and whenever possible littermate controls were used. To ensure optimal access of the dystrophic mice to water and food, cages were supplied with long-necked water bottles and wet food. All procedures were performed in accordance with the Swiss regulations for animal experimentation and under the required licenses.

Treatment of dy^W/mag mice with omigapil

Homozygous dy^W/mag were treated with 0.1 mg/kg omigapil dissolved in 0.5% ethanol as vehicle. For all experiments, treatment started at the age of 15 days. For the first week of drug treatment, omigapil was administered once daily by intraperitoneal injection. After weaning (3 weeks of age), omigapil was applied once daily by oral gavage. Age-matched animals treated with vehicle only were used as controls.

Masson trichrome, haematoxylin & eosin and immunostainings

Triceps brachii and *soleus* muscles were immersed in 7% gum Tragacanth (Sigma, St. Louis, MO, USA) and rapidly frozen in liquid nitrogen-cooled isopentane (−150°C). Cross-sections of 12 μm thickness were cut and collected on SuperFrost® Plus slides. General histology was performed using H & E staining. To visualize collagenous tissue, Masson's trichrome staining (Luna, 1968) was performed using Trichrome Stain (Masson) Kit (Sigma–Aldrich, HT-15). The antibodies used for immunofluorescence were purchased from the following commercial sources: Monoclonal mouse anti-rat dMyHC, monoclonal rat anti-mouse laminin-γ1 chain (Chemicon, MAB1914) and monoclonal rat anti-mouse F4/80 (Abcam, ab6640). Membrane-bound and extracellular epitopes were visualized with Alexa-488- or Alexa-594 conjugated wheat germ agglutinin (WGA; Molecular Probes). Appropriate secondary antibodies were: Cy3-conjugated (Jackson ImmunoResearch Laboratories), Alexa Fluor® 488-conjugated secondary antibodies (Molecular Probes) and TRITC-labelled streptavidin. Apoptotic myonuclei were detected by 'TdT-mediated dUTPbiotin nick end labelling' (TUNEL) using the '*In Situ* Cell Death Detection Kit, Fluorescein' according to the manufacturer's protocol (Roche Diagnostics Ltd). DAPI (4′,6′-Diamidino-2-phenylindole hydrochloride) was used to stain nuclei. Pictures of stained cross-sections were collected using a Leica DM5000B fluorescence microscope, a digital camera (F-View; Soft Imaging System), and analySIS® software (Soft Imaging System).

Histological quantifications

Mid-belly cross-sections of *triceps brachii* and *soleus* muscles were analysed. Muscle area, fibre number and fibre size distribution was evaluated using analySIS® software (Soft Imaging System). The muscle fibre size distribution was quantified on entire WGA-stained cross-sections using the minimum distance of parallel tangents at opposing particle borders (minimal 'Feret's diameter') as described (Briguet et al, 2004). Normalization of the number of fibres in each fibre diameter class of 5 μm was based on the total fibre number per muscle. Fibrotic area was evaluated on entire WGA-stained cross-sections, was normalized to muscle area and was expressed relative to controls. Fibres with centrally located nuclei (CNF) and regenerating dMyHC-positive fibres were counted in the entire WGA/DAPI-stained and dMyHC/laminin-γ1/DAPI stained cross-sections, respectively. Only TUNEL- and DAPI-positive nuclei located within muscle fibres were counted as apoptotic myonuclei. F4/80 staining allowed counting of macrophages in the entire cross-sections. In all histological quantification experiments, at least four mice of each testing group were analysed.

Notexin-induced muscle damage

Tibialis anterior of 6-week-old mice was injured by injection of 15 μl notexin (Sigma, 50 μg/ml) as described (Bentzinger et al, 2005). Mice were sacrificed 6 and 14 days post-injection and muscles were isolated and processed as described above.

Western blot

Triceps brachii muscles were homogenized in RIPA protein extraction buffer (Abcam). Equal amounts of protein were separated on 20% (Bcl2, 25 kD) or 12% (mini-agrin, double band ∼120 kD) SDS–PAGE and immunoblotted. Nitrocellulose membrane was incubated with antibody to human Bcl2 (CST#2872) and polyclonal rabbit anti-chick N25C95 mini-agrin (Ab 201), that was produced in-house (Gesemann et al, 1995). For detection, appropriate horse radish peroxidase-conjugated antibodies were used and immunoreactivity was visualized by the ECL detection method (Pierce).

Body condition and behavioural tests, creatine kinase assay

Overall disease score was assessed using a health score sheet that judges activity, appetite, posture, fur and eyes of 8-, 12- and 16-week-old mice. Scores: from 0 to 4 = good health: bright and active attitude; normal posture, movements, fur and eyes; 5–8 = fair health: Several measures are mildly affected; 9–11 = poor health: mouse is obviously sick (inactivity, small size, hunchback, severe uncoordinated movements, dull fur and eyes); 12–14 = death expected in near future: almost unable to move, small, thin, dehydrated, unkempt fur and matted eyes. Body weight was measured at the age of 8, 12 and 16 weeks. Locomotive behaviour was evaluated by placing the mice into a new cage and measuring motor activity (walking, digging and righting up) during 10 min (Moll et al, 2001). Grip strength was determined by measuring the time the animals can hold on a vertical grid. Cut-off time was 180 s. All values were normalized to values obtained from control animals. Blood levels of CK were determined with 2 μl of serum using the CK-NAC Liqui-UV kit (Rolf Greiner Biochemica). In omigapil-treated mice, body weight and death events were recorded daily. The body weight was recorded for each animal from day 15 (onset of the experiment) onwards. For each animal, the average weight gain per week was calculated.

In vitro muscle force assessment

Left and right EDL and *soleus* muscles of at least three 4-week-old mice per genotype were carefully dissected and mounted into a muscle testing setup (Heidelberg Scientific Instruments) to test force *in vitro*. By stimulation with a single electrical pulse (4 kHz, 15 Volt, 0.5 ms) using an AD Instruments converter, muscles were adjusted to the optimum length (L_0; mm) which is achieved when isometric twitch force is maximal (P_t; mN). Tetanus and force-frequency relationship were evaluated in response to 400 ms pulses at 10–120 Hz in EDL and

The paper explained

PROBLEM:

Congenital muscular dystrophies are early onset, often severe diseases of the skeletal muscle that are of heterogeneous genetic origin. MDC1A is the most prevalent form of those congenital muscular dystrophies and is caused by mutations in the gene encoding laminin-α2, which is one of the subunits of LM-211, a major component of the muscle basement membrane. MDC1A patients often cannot stand or walk, suffer from respiratory distress and eventually die in early childhood. There is no treatment option for those patients but recent years have seen quite some progress in the understanding of the disease mechanisms and preclinical studies have suggested a few new treatment options.

RESULTS:

This study is based on previous, preclinical experiments that established two independent ways to slow down disease progression in a mouse model for MDC1A, the dy^W/dy^W mice. The first option uses a miniaturized form of the extracellular matrix molecule agrin (mini-agrin), which is not homologous to LM-211, but shares binding properties with the protein that allow it to restore the mechanical linkage between muscle fibre and basement membrane. The second option uses inhibition of apoptosis, as muscle fibres in MDC1A undergo massive cell death because of their fragility. Although each treatment alone does not alleviate all of the dystrophic symptoms in mice, they both offer distinctive and interesting entry points for a possible treatment of MDC1A patients. We therefore examined in a mouse model for MDC1A whether the combination of both treatments would exert additive benefits and thus increase treatment efficacy.

We find that such a combined treatment with mini-agrin and apoptosis inhibition by either transgenic Bcl2 expression or application of the orally available apoptosis inhibitor omigapil indeed provides additive benefit on the disease progression in dy^W/dy^W mice. The side-by-side comparison also showed that mini-agrin treatment is superior to apoptosis inhibition, which is consistent with the notion that mini-agrin exerts its function at the early steps of the disease. The combination proved superior to single treatment with mini-agrin in preserving the number of muscle fibres and allowing improved survival of muscle fibres upon damage thereby improving muscle regeneration. Importantly, this improvement resulted in a marked increase in muscle force.

IMPACT:

Our work thus represents a proof-of-concept study showing that combination therapies might be beneficial for the treatment of MDC1A patients. Unfortunately, gene therapeutic approaches in patients (which could be used to apply mini-agrin) are still facing challenges. Thus, our work also suggests that the combination of pharmacological inhibition of apoptosis combined with low efficacy application of mini-agrin (e.g. injection of recombinant protein or low efficacy gene therapy) might still be a valuable option to improve the disease in MDC1A patients. The finding that muscle force is clearly improved by the combination treatment in the dy^W/dy^W mice further suggest that such a therapy might be particularly beneficial to improve muscle function and thus the mobility of MDC1A patients.

in response to 1100 ms pulses at 10–150 Hz in *soleus*. Maximum absolute isometric tetanic force (P_0) was determined from the plateau of the frequency–force relationship, which was typically achieved with 150 Hz for EDL, and for *soleus* muscles with 100 Hz. Since absolute P_0 is dependent upon muscle size, P_0 values were normalized for CSA [CSA = muscle mass/$L_0 \times 1.06$; (Brooks & Faulkner, 1988) and were expressed as specific force (sP_0; kN/m^2).

Statistical analysis

Quantitative data are expressed as mean ± SEM. To compare the different genotypes, *p*-values were calculated using the unpaired two-sample Student *t*-test assuming equal variances. Statistical analysis of values that were measured at two different time points used the two-way ANOVA test. Kaplan–Meier survival curves were generated and compared using the Peto–Peto Wilcoxon test.

Author contributions

SM designed, performed and evaluated most of the experiments; SL helped in the notexin experiments and RT helped to measure muscle force *in vitro*; ME and TM helped with the application of omigapil and helped with statistics; MAR designed and evaluated the experiments, and wrote the manuscript together with SM. All the authors read and commented on the manuscript.

Acknowledgements

We thank Dr Janice Dominov for generously providing the mice expressing human Bcl2 in skeletal muscles. The *in vitro* force measurements on isolated muscles were performed in the laboratories of Dr Francesco Zorzato. We thank Teppo Huttunen for many helpful discussions. This work was supported by the 'Muscular Dystrophy Association (MDA)', 3300 East Sunrise Drive, Tucson, AZ 85718, the Swiss Foundation for Research on Muscle Disease and the Cantons of Basel-Stadt and Baselland.

Supporting information is available at EMBO Molecular Medicine online.

The authors declare that they have no conflict of interest.

For more information

Patient organization Cure CMD:
http://curecmd.org/

Muscular Dystrophy Association:
http://www.mdausa.org/

Swiss Foundation for Research on Muscle Diseases:
http://www.ssem.ch

TREAT-NMD Neuromuscular Network:
http://www.treat-nmd.eu

References

Bentzinger CF, Barzaghi P, Lin S, Ruegg MA (2005) Overexpression of mini-agrin in skeletal muscle increases muscle integrity and regenerative capacity in laminin-alpha2-deficient mice. FASEB J 19: 934-942

Bezakova G, Ruegg MA (2003) New insights into the roles of agrin. Nat Rev Mol Cell Biol 4: 295-308

Briguet A, Courdier-Fruh I, Foster M, Meier T, Magyar JP (2004) Histological parameters for the quantitative assessment of muscular dystrophy in the mdx-mouse. Neuromuscul Disord 14: 675-682

Brooks SV, Faulkner JA (1988) Contractile properties of skeletal muscles from young, adult and aged mice. J Physiol 404: 71-82

Bulyakova NV, Azarova VS (2006) Regeneration of skeletal muscles and state of thymus in gamma-irradiated rats under laser therapy of the area of muscle trauma. Minim Invasive Ther Allied Technol 15: 277-285

Burkin DJ, Kaufman SJ (1999) The alpha7beta1 integrin in muscle development and disease. Cell Tissue Res 296: 183-190

Charge SB, Brack AS, Bayol SA, Hughes SM (2008) MyoD- and nerve-dependent maintenance of MyoD expression in mature muscle fibres acts through the DRR/PRR element. BMC Dev Biol 8: 5

Collins J, Bonnemann CG (2010) Congenital muscular dystrophies: toward molecular therapeutic interventions. Curr Neurol Neurosci Rep 10: 83-91

Colognato H, Yurchenco PD (1999) The laminin alpha2 expressed by dystrophic dy(2J) mice is defective in its ability to form polymers. Curr Biol 9: 1327-1330

Colognato H, Yurchenco PD (2000) Form and function: the laminin family of heterotrimers. Dev Dyn 218: 213-234

Denzer AJ, Brandenberger R, Gesemann M, Chiquet M, Ruegg MA (1997) Agrin binds to the nerve-muscle basal lamina via laminin. J Cell Biol 137: 671-683

Dominov JA, Kravetz AJ, Ardelt M, Kostek CA, Beermann ML, Miller JB (2005) Muscle-specific BCL2 expression ameliorates muscle disease in laminin {alpha}2-deficient, but not in dystrophin-deficient, mice. Hum Mol Genet 14: 1029-1040

Erb M, Meinen S, Barzaghi P, Sumanovski LT, Courdier-Fruh I, Ruegg MA, Meier T (2009) Omigapil ameliorates the pathology of muscle dystrophy caused by laminin-alpha2 deficiency. J Pharmacol Exp Ther 331: 787-795

Gesemann M, Denzer AJ, Ruegg MA (1995) Acetylcholine receptor-aggregating activity of agrin isoforms and mapping of the active site. J Cell Biol 128: 625-636

Gesemann M, Brancaccio A, Schumacher B, Ruegg MA (1998) Agrin is a high-affinity binding protein of dystroglycan in non-muscle tissue. J Biol Chem 273: 600-605

Girgenrath M, Dominov JA, Kostek CA, Miller JB (2004) Inhibition of apoptosis improves outcome in a model of congenital muscular dystrophy. J Clin Invest 114: 1635-1639

Girgenrath M, Beermann ML, Vishnudas VK, Homma S, Miller JB (2009) Pathology is alleviated by doxycycline in a laminin-alpha2-null model of congenital muscular dystrophy. Ann Neurol 65: 47-56

Hayashi YK, Tezak Z, Momoi T, Nonaka I, Garcia CA, Hoffman EP, Arahata K (2001) Massive muscle cell degeneration in the early stage of merosin-deficient congenital muscular dystrophy. Neuromuscul Disord 11: 350-359

Kuang W, Xu H, Vachon PH, Engvall E (1998a) Disruption of the *lama2* gene in embryonic stem cells: laminin alpha 2 is necessary for sustenance of mature muscle cells. Exp Cell Res 241: 117-125

Kuang W, Xu H, Vachon PH, Liu L, Loechel F, Wewer UM, Engvall E (1998b) Merosin-deficient congenital muscular dystrophy. Partial genetic correction in two mouse models. J Clin Invest 102: 844-852

Kuang W, Xu H, Vilquin JT, Engvall E (1999) Activation of the *lama2* gene in muscle regeneration: abortive regeneration in laminin alpha2-deficiency. Lab Invest 79: 1601-1613

Langenbach KJ, Rando TA (2002) Inhibition of dystroglycan binding to laminin disrupts the PI3K/AKT pathway and survival signaling in muscle cells. Muscle Nerve 26: 644-653

Laprise P, Poirier EM, Vezina A, Rivard N, Vachon PH (2002) Merosin–integrin promotion of skeletal myofiber cell survival: differentiation state-distinct involvement of p60Fyn tyrosine kinase and p38alpha stress-activated MAP kinase. J Cell Physiol 191: 69-81

Laprise P, Vallee K, Demers MJ, Bouchard V, Poirier EM, Vezina A, Reed JC, Rivard N, Vachon PH (2003) Merosin (laminin-2/4)-driven survival signaling: complex modulations of Bcl-2 homologs. J Cell Biochem 89: 1115-1125

Luna L (1968) *Manual of Histologic Staining Methods of the Armed Forces Institute of Pathology*. New York, McGraw-Hill: pp 94-95.

Meinen S, Barzaghi P, Lin S, Lochmuller H, Ruegg MA (2007) Linker molecules between laminins and dystroglycan ameliorate laminin-alpha2-deficient muscular dystrophy at all disease stages. J Cell Biol 176: 979-993

Miller R, Bradley W, Cudkowicz M, Hubble J, Meininger V, Mitsumoto H, Moore D, Pohlmann H, Sauer D, Silani V, *et al* (2007) Phase II/III randomized trial of TCH346 in patients with ALS. Neurology 69: 776-784

Miyagoe Y, Hanaoka K, Nonaka I, Hayasaka M, Nabeshima Y, Arahata K, Takeda S (1997) Laminin alpha2 chain-null mutant mice by targeted disruption of the *Lama2* gene: a new model of merosin (laminin 2)-deficient congenital muscular dystrophy. FEBS Lett 415: 33-39

Miyagoe-Suzuki Y, Nakagawa M, Takeda S (2000) Merosin and congenital muscular dystrophy. Microsc Res Tech 48: 181-191

Moll J, Barzaghi P, Lin S, Bezakova G, Lochmuller H, Engvall E, Muller U, Ruegg MA (2001) An agrin minigene rescues dystrophic symptoms in a mouse model for congenital muscular dystrophy. Nature 413: 302-307

Olanow CW, Schapira AH, LeWitt PA, Kieburtz K, Sauer D, Olivieri G, Pohlmann H, Hubble J (2006) TCH346 as a neuroprotective drug in Parkinson's disease: a double-blind, randomised, controlled trial. Lancet Neurol 5: 1013-1020

Olive M, Ferrer I (2000) Bcl-2 and bax immunohistochemistry in denervation–reinnervation and necrosis-regeneration of rat skeletal muscles. Muscle Nerve 23: 1862-1867

Qiao C, Li J, Zhu T, Draviam R, Watkins S, Ye X, Chen C, Xiao X (2005) Amelioration of laminin-alpha2-deficient congenital muscular dystrophy by somatic gene transfer of miniagrin. Proc Natl Acad Sci USA 102: 11999-12004

Shefer G, Partridge TA, Heslop L, Gross JG, Oron U, Halevy O (2002) Low-energy laser irradiation promotes the survival and cell cycle entry of skeletal muscle satellite cells. J Cell Sci 115: 1461-1469

Tapscott SJ, Lassar AB, Weintraub H (1992) A novel myoblast enhancer element mediates MyoD transcription. Mol Cell Biol 12: 4994-5003

Tome FM, Fardeau M (1998) Hereditary inclusion body myopathies. Curr Opin Neurol 11: 453-459

Vachon PH, Loechel F, Xu H, Wewer UM, Engvall E (1996) Merosin and laminin in myogenesis; specific requirement for merosin in myotube stability and survival. J Cell Biol 134: 1483-1497

Vachon PH, Xu H, Liu L, Loechel F, Hayashi Y, Arahata K, Reed JC, Wewer UM, Engvall E (1997) Integrins (alpha7beta1) in muscle function and survival. Disrupted expression in merosin-deficient congenital muscular dystrophy. J Clin Invest 100: 1870-1881

